Investigation of Optical Properties of Nanoscale Heterostructure GaAsSb/AlGaAsSb for Mid Infrared Region

Divya Bharadwaj, J.P. Vijay, Monika Mathur
Department of Electronics & Communication Engineering, Swami Keshvanand Institute of Technology, Management & Gramothan, Jaipur, India
Email: divyabharadwaj4482@gmail.com, jayprakash.vijay@skit.ac.in, monikamathur@skit.ac.in
Received 29.06.2022, received in revised form 03.08.2022, accepted 12.08.2022
DOI: *10.47904/IJSKIT.12.2.2026.21-25*

***Abstract*- The type-I nanoscale heterostructure $Al_{0.3}Ga_{0.7}As_{0.03}Sb_{0.97}$/ $GaAs_{0.6}Sb_{0.4}$/ $Al_{0.3}Ga_{0.7}As_{0.03}Sb_{0.97}$ grown on GaSb substrate at room temperature (300K) has been investigated in this paper. The injected carrier concentration has been set at 2.5 x $10^{12}/cm^2$. The design is modelled with k.p technique using 4x4 Luttinger-Kohn Hamiltonian model with conduction band. The effects due to external temperature and strain have also been investigated. The energy wavefunctions, dispersion profile, optical gain etc have been computed for lasing wavelengths in mid infrared region.**

Keywords- AlGaAsSb, GaAsSb, Quantum well, Optical gain, 4x4 L-K Hamiltonian

1. INTRODUCTION

The mid infrared region spans the wavelength range between 2-12μm of the electromagnetic spectrum, corresponding to energy between 0.62eV-0.1eV [1]. It is a technologically significant spectral region for imaging, sensing and communication and past decade has seen a rise in mid-infrared optoelectronics. Mid infrared semiconductor lasers with fixed or tunable wavelengths are used in infrared spectroscopy including the environmental gas monitoring and breath analysis, microscopy, minimally invasive laser surgery etc [2-6].

The III-Sb multinary materials have a wide bandgap range, ranging from 0.1 to 2 eV, and are approximately lattice matched to GaSb. The AlGaAsSb and GaInAsSb quaternary alloys, which constitute the foundation of MIR III-Sb laser diodes, have large and narrow bandgaps, respectively. The carrier mobilities of III-Sbs are high. Among all compound semiconductors, InSb and GaSb have the highest electron and hole mobilities, respectively. [7-9]

These characteristics distinguish III–Sb compounds from other III–V semiconductors. They provide unique potential for bandgap and band offset engineering, as well as device design. They enable the creation of artificial, man-made materials with effective bandgaps that may be adjusted by design over the whole spectrum from near-IR to long-IR and THz. Hyper-frequency transistors, high efficiency solar cells and imaging IR photodetectors are among the technologies that the III-Sb technology is ideally suited to produce. It's also the technology of choice for MIR laser development [10-12].

2. HETEROSTRUCTURE DESIGN

The designed nanoscale heterostructure AlGaAsSb/ GaAsSb/AlGaAsSb consist of quantum well of n-type GaAsSb material and p-type AlGaAsSb material as barrier layer. The heterostructure is modelled on GaSb substrate at room temperature. The band structure of the materials AlGaAsSb and GaAsSb are shown in figure 1 and 2, thereby giving the energy band alignment as in figure 3.

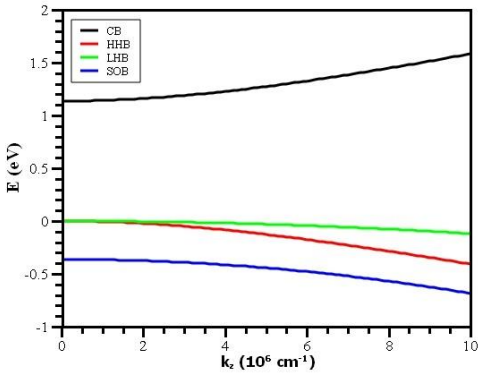

Figure 1: Bulk band structure of AlGaAsSb

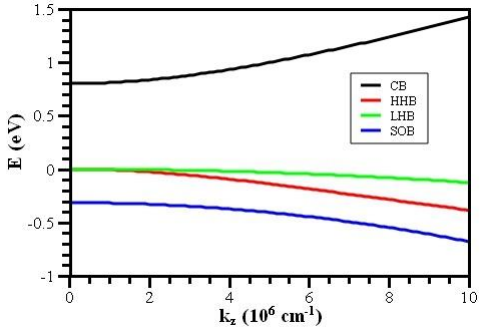

Figure 2: Bulk band structure of GaAsSb

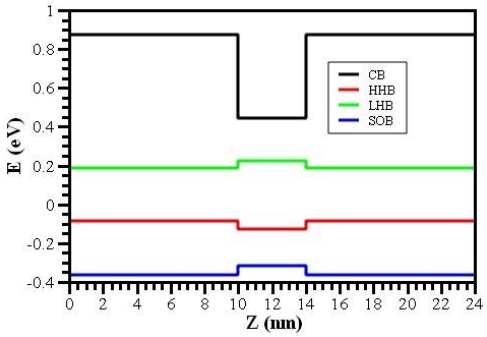

Figure 3: Band alignment of energy bands of AlGaAsSb/GaAsSb/AlGaAsSb

The materials are chosen based on their capacity to generate light in the MIR wavelength as a requirement. The material choices, material composition and layer widths are the important criteria that influence the heterostructure design. After multiple computations, the width of the layers is chosen to maximise carrier confinement and efficient recombination of charge carriers, which results to an increase in optical gain at the appropriate MIR wavelengths.

In the proposed heterostructure, the widths of the quantum well layer is 4nm and the barrier layer is 10nm. The compositions of the materials are selected according to the lattice matching and direct energy bandgap. The lattice matching for AlGaAsSb with GaSb is given by the following equation (i) [13,14]

$$y = \frac{0.0396x}{0.4426+0.0318x}, \ (0 \le x \le 1) \qquad \text{(i)}$$

The bandgap energy plot of AlGaAsSb is shown in figure 4 which is computed from the following equations [15],

$$E_{Direct} = 0.704925 + 1.0809x + 0.47x^2 \qquad \text{(ii)}$$

$$E_{Indirect} = 1.04088 + 0.55525x \qquad \text{(iii)}$$

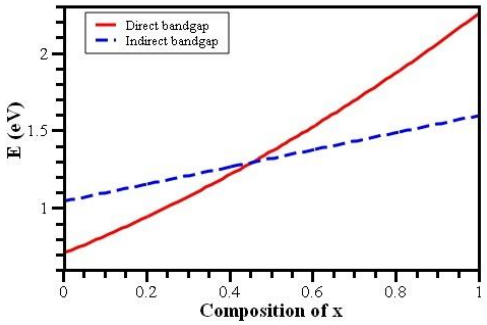

Figure 4: Direct and indirect bandgap energy of AlGaAsSb

From figure 4 and equations (ii) and (iii), it can be shown that AlGaAsSb lattice matched to GaSb will transition from direct energy bandgap to indirect energy bandgap at x~0.45.

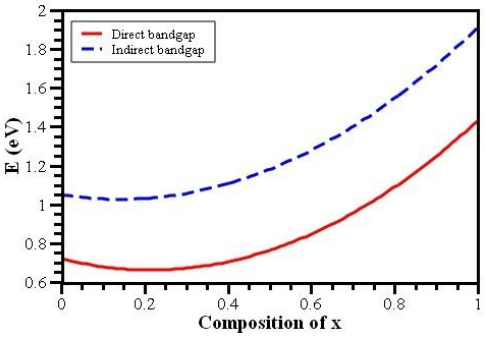

Figure 5: Direct and indirect bandgap energy of GaAsSb

The bandgap energy of GaAsSb is computed by equations (iv) and (v) and plotted in figure 5 [16]. It can be seen that GaAsSb is a direct bandgap energy material.

$$E_{Direct} = 0.72 - 0.54x + 1.25x^2 \qquad \text{(iv)}$$

$$E_{Indirect} = 1.05 - 0.34x + 1.2x^2 \qquad \text{(v)}$$

From the above computations the composition of the material is selected as $Al_{0.3}Ga_{0.7}As_{0.03}Sb_{0.97}/GaAs_{0.6}Sb_{0.4}/Al_{0.3}Ga_{0.7}As_{0.03}Sb_{0.97}$.

3. RESULTS AND DISCUSSION

In this work, the type-I nanoscale heterostructure $Al_{0.3}Ga_{0.7}As_{0.03}Sb_{0.97}/GaAs_{0.6}Sb_{0.4}/Al_{0.3}Ga_{0.7}As_{0.03}Sb_{0.97}$ on GaSb substrate is modelled and investigated to emit radiation in the mid infrared region. The designed heterostructure has also been investigated for dependency of emission wavelength and optical gain on externally applied temperature and strain.

The calculations are performed using k.p technique using 4x4 Luttinger-Kohn model with conduction band. The 4x4 L-K Hamiltonian is solved to compute the energy wavefunctions, quantized energies and carrier densities [17-19].

Figure 6 depicts the acquired localization densities in relation to the calculated wave functions at room temperature and without the presence of external strain. The quantum well region of GaAsSb material has the highest electron density as well the highest hole density. The electron-hole recombination takes place between carriers associated with the quantum well layer which confirms that the heterostructure is of type-I [20-22].

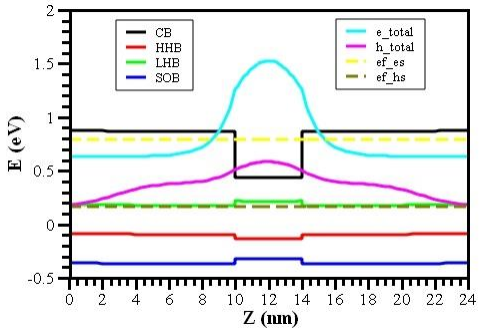

Figure 6: Wavefunction showing electrons and holes density concentration in type-I AlGaAsSb/GaAsSb/AlGaAsSb heterostructure

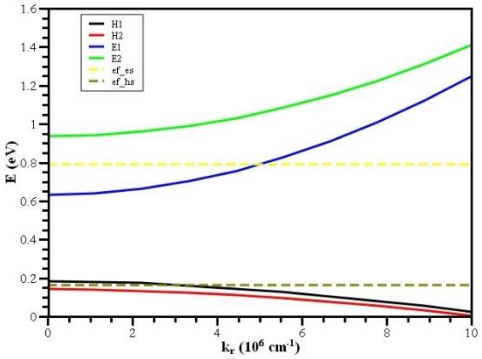

Figure 7: Energy dispersion characteristics for AlGaAsSb/GaAsSb/AlGaAsSb heterostructure

The sub-band dispersion curve of the heterostructure is shown in figure 7. The light holes play the primary role in the inter sub-band optical transitions, which become responsible for the optical gain characteristics of the heterostructure, since the most probabilistic inter sub-band transition takes place between E1 and LH1 or E1 and LH2.

In figure 8, the optical gain characteristic of the type-I $Al_{0.3}Ga_{0.7}As_{0.03}Sb_{0.97}$/ $GaAs_{0.6}Sb_{0.4}$/ $Al_{0.3}Ga_{0.7}As_{0.03}Sb_{0.97}$ quantum well nanoscale heterostructure has been plotted as a function of energy. The magnitude of the optical gain achieved at peak is of order 7807/cm corresponding to 0.4606eV photonic energy resulting from optical transition between electron and hole sub-bands. The lasing wavelength of 2692nm is thus achieved at room temperature.

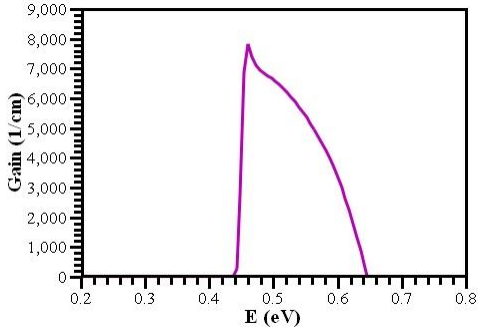

Figure 8: Optical gain characteristics of AlGaAsSb/GaAsSb/ AlGaAsSb nanoscale heterostructure at room temperature

It has been discovered that applying external temperature and strain may modify material characteristics like the lattice constant and bandgap energy by distorting the electronic structure of the material. The effects of external temperature and strain are examined in order to analyse the tunability of the optical gain for the modelled heterostructure [23].

The temperature dependence of the bandgap energy is taken into account according to the empirical Varshni expression [24] given below,

$$E_g(T) = E_g(0) - \frac{\alpha T^2}{T+\beta} \qquad \text{(vi)}$$

where α and β are adjustable parameters, $E_g(0)$ is bandgap energy at zero temperature. This equation illustrates that the bandgap energy decreases as there is increase in temperature. The figure 9 depicts the variation of optical gain spectra on application of external temperature as a function of photonic energy. From the figure 9 it can be observed that with the increase in temperature: (a) the optical gain decreases, (b) photonic energy decreases, (c) lasing wavelength shifts to higher values. When the temperature is increased, the radiative recombination decreases and non-radiative recombination increases resulting into the reduction of optical gain. The table 1 gives the computed values of optical gain along with corresponding lasing wavelength and energy on application of external temperature.

Table 1: Variation of energy, lasing wavelength and optical gain corresponding to external temperature

Temperature (K)	E (eV)	λ (nm)	Gain (1/cm)
100	0.52727	2352	9112.403
200	0.49697	2495	8743.025
300	0.46060	2692	7807.544
400	0.42424	2923	6756.485

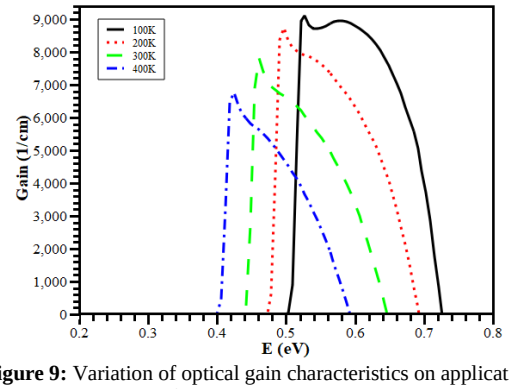

Figure 9: Variation of optical gain characteristics on application of external temperature

The effect of strain on the heterostructure can be internal or external. The internal strain is due to the

lattice mismatch in the heterostructure material layers. Due to application of external it is possible to accomplish population inversion with a lower injected carrier density because when strain is applied it lowers the effective mass at the top of the valence band. The 3-D symmetry of the bulk crystal is distorted by external strain, matching it closer to the 1-D symmetry of the laser beam. As a result, a greater percentage of the carriers in the active region directly contribute to optical gain. For the designed heterostructure the external uniaxial strain is investigated in [100], [110] and [001] directions [25-27].

Figures 10, 11 and 12 displays the optical gain and tuning range for MIR lasing wavelengths when external strains of 2 GPa, 4 GPa, and 6 GPa are applied at room temperature (300K) in directions [100], [110] and [001] respectively.

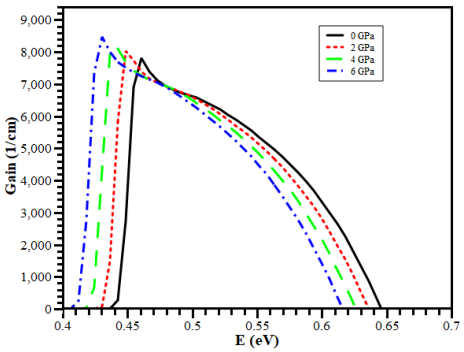

Figure 10: Variation of optical gain characteristics on application of external uniaxial strain in direction [100]

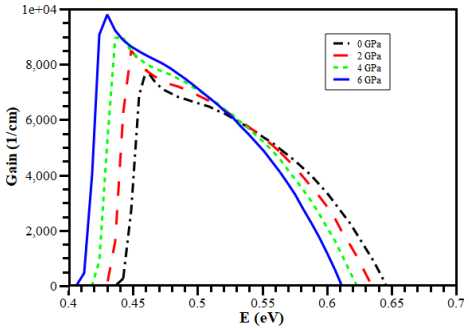

Figure 11: Variation of optical gain characteristics on application of external uniaxial strain in direction [110]

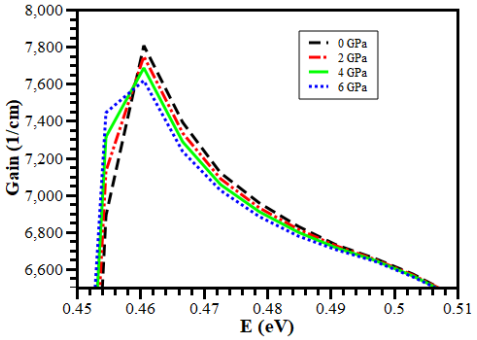

Figure 12: Variation of optical gain characteristics on application of external uniaxial strain in direction [001]

It can be seen from figure 10, that on application of uniaxial strain in direction [110], there is improvement in optical gain. As the strain is increased, there is increase in optical gain and lasing wavelength while the photonic energy is decreased. Similarly, from figure 12 it can be observed that on application of uniaxial strain in direction [100], there is major increase in optical gain as compared to strain in direction [110]. The lasing wavelength is also increased while the photonic energy is decreased. Table 2 compares the optical gains achieved with strain in [100] and [110] direction. But on application of uniaxial strain in direction [001], there is no improvement in optical gain and the photonic energy and lasing wavelength remain same as that present at room temperature.

The attained optical gain is quite high as compared to previously reported heterostructures:

(a) Type-I InGaAlAs/InP (optical gain 5500/cm at 1.55μm) [28],

(b) Type-I $Al_{0.45}Ga_{0.55}As$/ $GaAs_{0.84}P_{0.16}$ heterostructure (optical gain 3000/cm) [29],

(c) Type-II InGaAs/ InAs/ GaAsSb heterostructure (optical gain 7500/cm) [30],

(d) Type-I $In_{0.29}Ga_{0.71}As_{0.99}N_{0.01}$/GaAs heterostructure (optical gain ~ 2100/cm) [31],

(e) Type-I GaSbBi/ GaSb heterostructure (optical gain 3000/cm at 2700nm) [32]

Table 2: Comparison of optical gain achieved on application of uniaxial strain in directions [100] and [110]

Strain (GPa)	E (eV)	λ (nm)	Gain in [110] direction (1/cm)	Gain in [100] direction (1/cm)
0	0.4606	2692	7807.54	7807.54
2	0.4484	2765	8026.61	8492.09
4	0.4424	2803	8105.01	8960.53
6	0.4303	2882	8472.43	9793.73

4. CONCLUSION

The type-I nanoscale heterostructure $Al_{0.3}Ga_{0.7}As_{0.03}Sb_{0.97}/GaAs_{0.6}Sb_{0.4}/Al_{0.3}Ga_{0.7}As_{0.03}Sb_{0.97}$ on GaSb substrate has been investigated in this paper. The lasing wavelength of 2692nm corresponding to photonic energy 0.4604eV was achieved at room temperature with high optical gain of order 7807/cm. The heterostructure is simulated through k.p technique using 4x4 Luttinger Kohn Hamiltonian model with conduction band. The effects of application of external temperature and strain have also been investigated. The modelled tunable heterostructure can be utilized in the mid infrared region applications including environmental monitoring.

REFERENCES

[1] Tournie, Eric, and Alexei N. Baranov, "Mid-infrared semiconductor lasers: a review", Elsevier Semiconductors and Semimetals, (2012), vol. 86, 183-226.

[2] J. Haas and B. Mizaikoff, "Advances in mid-infrared spectroscopy for chemical analysis". Annual Review of Analytical Chemistry, (2016), Vol. 9, 1, 45-68.

[3] F.K. Tittel et al., "Mid-infrared Laser Based Gas Sensor Technologies for Environmental Monitoring, Medical Diagnostics, Industrial and Security Applications", Terahertz and Mid Infrared Radiation: Detection of Explosives and CBRN (Using Terahertz), Dordrecht (Netherlands), (2014), 153-165.

[4] B. Henderson et al., "Laser spectroscopy for breath analysis: towards clinical implementation", Applied physics B, (2018), vol. 124, 8, 1-21.

[5] M. A. Pleitez et al., "Label-free metabolic imaging by mid-infrared optoacoustic microscopy in livings cells", Nature biotechnology, (2020), vol. 38, 3, 293-296.

[6] S. Amini-Nik et al., "Ultrafast Mid-IR laser scalpel: Protein signals of the fundamental limits to minimally invasive surgery", PloS one, (2010), vol. 5, 9, e13053

[7] Sai-Halasz, G. A., R. Tsu, and L. Esaki, "A new semiconductor superlattice", Applied Physics Letters, (1977), vol. 30, 12, 651-653.

[8] Smith, D. L., and C. Mailhiot, "Proposal for strained type II superlattice infrared detectors", Journal of Applied Physics, (1987), vol. 62, 6, 2545-2548.

[9] I. Vurgaftman, J.R. Meyer, L.R. Ram-Mohan, "Band parameters for III–V compound semiconductors and their alloys", Journal of Applied Physics, (2001), vol. 89, 11, 5815-5875.

[10] Luna E, Satpati B, Rodriguez JB, Baranov AN, Tournié E, Trampert A., "Interfacial intermixing in InAs/GaSb short-period-superlattices grown by molecular beam epitaxy", Applied Physics Letters, (2010), vol. 96, 2, 021904.

[11] Satpati, B., Rodriguez, J. B., Trampert, A., Tournié, E., Joullié, A., & Christol, P., "Interface analysis of InAs/GaSb superlattice grown by MBE", Journal of Crystal Growth, (2007), vol. 301-302, 889-892.

[12] Szmulowicz, F., Haugan, H., Brown, G., Mahalingam, K., Ullrich, B., Munshi, S. R., & Grazulis, L., "Interfaces as design tools for short-period InAs/GaSb type-II superlattices for mid-infrared detectors", Opto-Electronics Review, (2006), vol. 14, 1, 69-75.

[13] Adachi S., "Band gaps and refractive indices of AlGaAsSb, GaInAsSb, and InPAsSb: Key properties for a variety of the 2~4μm optoelectronic device applications", Journal of Applied Physics, (1987), vol. 61, 10, 4869–4876.

[14] Ait Kaci, H., D. Boukredimi, and M. Mebarki, "Band Discontinuities of Perfectly Lattice-Matched GaSb (n)/GaAlAsSb (p)/GaSb (p) Double Heterojunction", Physica Status Solidi (a), (1997), vol. 163, 1, 101-106.

[15] S. Adachi, "Properties of Group-IV, III-V and II-VI Semiconductors",1st edition, John Wiley & Sons, Chichester, (2005).

[16] Adachi, S., "Handbook on physical properties of semiconductors", 1st edition, Springer Science & Business Media, New York, (2004).

[17] Kane E. O., "The k• p Method", Elsevier Semiconductors and semimetals, (1966), vol. 1, 75-100.

[18] Luttinger, J. M., & Kohn, W., "Motion of electrons and holes in perturbed periodic fields", Physical Review, (1955), 97, 4, 869.

[19] Luttinger, J. M., "Quantum theory of cyclotron resonance in semiconductors: General theory", Physical Review, (1956), vol. 102, 4, 1030.

[20] M. F. H. Schuurmans and G. W. 't Hooft, "Simple calculations of confinement states in a quantum well," Physical Review: B, (1985), vol. 31, 12, 8041–8048.

[21] R. Winkler and U. Rossler, "General approach to the envelope-function approximation based on a quadrature method," Physical Review: B, (1993), vol. 48, 12, 8918–8927.

[22] A. T. Meney, B. Gonul, and E. P. O'Reilly, "Evaluation of various approximations used in the envelope-function method," Physical Review: B, (1994), vol. 50, 15, 10893–10904.

[23] S. L. Chuang, *"Physics of Optoelectronic Devices"*, 1st edition, John Wiley & Sons, New York, (1995).

[24] Y. P. Varshni, "Temperature dependence of the energy gap in semiconductors," Elsevier Physica, (1976), vol. 34, 1, 149–154.

[25] Lee, J., & Vassell, M. O., "Effects of uniaxial stress on hole subbands in semiconductor quantum wells. I. Theory", Physical Review: B, (1988), vol. 37, 15, 8855

[26] G. L. Bir and G. E. Pikus, eds., "Symmetry and Strain-Induced Effects in Semiconductors", 1st edition, John Wiley & Sons, New York, (1974).

[27] G. Bastard, *"Wave mechanics applied to semiconductor heterostructures"*, 1st edition, Halsted Press, New York, (1988).

[28] Alvi, P. A, "Strain-induced non-linear optical properties of straddling-type indium gallium aluminum arsenic/indium phosphide nanoscale-heterostructures", Elsevier Materials Science in Semiconductor Processing, (2015), vol. 31, 106-115.

[29] Nirmal, H.K., Anjum, S.G., Lal, P., Rathi, A., Dalela, S., Siddiqui, M.J., Alvi, P.A., "Field effective band alignment and optical gain in type-I Al0.45Ga0.55As/ GaAs0.84P0.16 nano-heterostructures", Optik, (2016), vol. 127, 18, 7274–7282.

[30] Bhardwaj, G., Yadav, N., Anjum, S.G., Siddiqui, M.J., Alvi, P.A., "Uniaxial strain induced optical properties of complex type-II InGaAs/InAs/GaAsSb nano-scale heterostructure", Optik, (2017), vol. 146, 8–16.

[31] Sandhya, K., Bhardwaj, G., Dolia, R., Lal, P., Kumar, S., Dalela, S., Rahman, F., Alvi, P.A., "Optimization of optical characteristics of In0.29Ga0.71As0.99N0.01/GaAs straddled nano-heterostructure", Opto-Electronics Review, (2018), vol, 26, 3, 210–216

[32] Ammar, I., Sfina, N., & Fnaiech, M., "Optical gain and threshold current density for mid-infrared GaSbBi/GaSb quantum-well laser structure", Materials Science and Engineering: B, (2021), 266, 115056.